Chemical Engineering Journal 523 (2025) 168035

Contents lists available at ScienceDirect

Chemical Engineering Journal

journal homepage: www.elsevier.com/locate/cej

Scaling up microbial electrolysis cells (MECs) for hydrogen production: Design, construction and operation of a 1 m^3 pilot plant in an urban wastewater treatment plant

Oscar Guerrero-Sodric, Juan Antonio Baeza *, Albert Guisasola

GENOCOV, Department of Chemical, Biological and Environmental Engineering, School of Engineering, Universitat Autònoma de Barcelona, 08193, Bellaterra, Spain

ARTICLE INFO

Keywords:
Bioelectrochemical systems
hydrogen
microbial electrochemical technology
microbial electrolysis cell
pilot scale
wastewater treatment

ABSTRACT

Microbial electrolysis cells (MECs) are considered a breakthrough technology in the water-energy nexus frame due to the good results obtained at lab-scale conditions: organic matter degradation with low sludge production and energy recovery as hydrogen. However, the scaling-up of these systems has found significant hurdles and the lab-scale performance has not been achieved at a higher scale. This study comprehensively details the design, construction, and operation of a 1 m^3 MEC pilot plant integrated into an urban wastewater treatment plant (WWTP) and fed with primary effluent. The experimental trials conducted showcased the MEC performance under varying operational conditions, achieving a maximum organic matter removal efficiency of 51 % and continuous hydrogen production at a maximum rate of 8.59 L m^{-2} d^{-1} (0.094 m^3 m^{-3} d^{-1}) with synthetic wastewater and 7.29 L m^{-2} d^{-1} (0.042 m^3 m^{-3} d^{-1} at full capacity, 15 cassettes) with real urban primary effluent. These results are comparable to those obtained in pilot MEC at smaller scales (~100 L), demonstrating a good scalability of the proposed prototype. A techno-economic assessment was performed to evaluate the commercial potential of the pilot MEC, considering factors such as revenue from hydrogen production, electricity consumption costs and capital expenses. The outcomes of this study represent a significant advancement in the scale-up of MECs, offering valuable insights into the challenges and opportunities associated with real-world implementation. Further improvements should focus on minimizing material costs, hydrogen leakages and voltage losses to enhance scalability, as well as exploring the applicability of MECs in niches other than urban WWTP.

1. Introduction

Global energy demand is persistently rising, driven by population growth, industrialization, and urbanization. This demand is largely met by carbon-intensive sources, including coal, oil, and natural gas, which contribute significantly to climate change, air pollution, and the depletion of natural resources [1]. Addressing these critical issues requires an urgent shift toward sustainable energy alternatives. Within this framework, the wastewater industry is beginning to recognize domestic wastewater not simply as waste but as a potential resource for energy and nutrient recovery. In terms of energy recovery, previous studies suggested an internal chemical energy content in wastewater of approximately 15 kJ per gram of chemical oxygen demand (COD) [2]. Traditional methods, such as anaerobic digestion, have long been used to convert organic matter in wastewater into biogas, primarily methane. Combined heat and power (CHP) systems are often employed in tandem with anaerobic digestion, capturing energy from both the heat and electricity produced during the process. These technologies have paved the way for a circular approach to wastewater management, integrating energy recovery with treatment.

More recently, microbial electrochemical technologies (METs) have gained attention as advanced, efficient technologies for energy recovery from wastewater. METs exploit the unique abilities of electroactive microorganisms (exoelectrogens), which catalyse redox reactions on the surface of an electrode directly through their metabolic processes. This biocatalysis enables METs to simultaneously recover energy or nutrients while treating wastewater. For instance, in microbial electrolysis cells (MECs), a type of MET, hydrogen gas (H_2) can be produced from wastewater under a certain applied potential (ΔV). H_2 production occurs at the cathode while exoelectrogens oxidize organic compounds at the anode, producing electrons and protons. This H_2 can be used for

* Corresponding author.
E-mail addresses: Oscar.Guerrero@uab.cat (O. Guerrero-Sodric), JuanAntonio.Baeza@uab.cat (J.A. Baeza), Albert.Guisasola@uab.cat (A. Guisasola).

https://doi.org/10.1016/j.cej.2025.168035
Received 23 June 2025; Received in revised form 15 August 2025; Accepted 2 September 2025
Available online 7 September 2025

Abbreviations

AEM	Anion exchange membrane
BES	Bioelectrochemical system
CAPEX	Capital expenditure
CE	Coulombic efficiency
CHP	Combined heat and power
COD	Chemical oxygen demand
COD_I	Inlet soluble chemical oxygen demand
COD_O	Outlet soluble chemical oxygen demand
COD_S	Soluble chemical oxygen demand
E_C	Energy consumption (electrical input)
E_P	Energy production (energy in produced H_2)
EPDM	Ethylene propylene diene monomer
GC	Gas chromatography
HER	Hydrogen evolution reaction
HRT	Hydraulic retention time
j	Current density
KPI	Key performance indicator
MEC	Microbial electrolysis cell
MET	Microbial electrochemical technologies
NPV	Net present value
OLR	Organic loading rate
ORR	Organic removal rate
PR	Price ratio (hydrogen price / electricity price, in kWh kg^{-1} H_2)
PVC	Polyvinyl chloride
r_{CAT}	Cathodic gas recovery
r_E	Energy recovery
SS	Stainless-steel
S/V	Projected anode surface area to reactor volume ratio (m^2 m^{-3})
SWW	Synthetic wastewater
T	Temperature
UWW	Urban wastewater
VSS	Volatile suspended solids
WWTP	Wastewater treatment plant
ΔV	Applied potential
σ	Electrical conductivity

multiple purposes, theoretically offering economic benefits and contributing to a reduction in greenhouse gas emissions if implemented on a large scale [3].

In fact, evidence from lab-scale research has validated the potential of MECs: typical lab-scale MEC set-ups can operate with low ΔV (<0.7 V) and yield high current densities (>2 A m^{-2}) [4,5], H_2 production rates (>1.3 m^3 m^{-3} d^{-1}) [6], and COD removal efficiencies (>95 %) [7]. However, the widespread adoption of MECs is hindered by the technical challenges associated with their scale-up, and the lack of pilot-scale research further hampers the transition to large-scale implementation. Particularly, most studies about MECs for wastewater treatment have been conducted with anodic volumes lower than 1 L [8]. The first pilot-scale MEC fed with wastewater was reported by [9] in a 1 m^3 single-chamber reactor. Although it was a visionary attempt to demonstrate MEC performance for real-world applications, the results were not satisfactory, and the initial low hydrogen (H_2) production was replaced by methane production. Subsequent pilot-scale studies (>100 L) have used double-chamber configurations to reduce methanogenesis and enhance hydrogen yield. Up to date, the largest reported double-chamber MEC had an anolyte volume of 135–150 L and was fed with synthetic, urban and industrial wastewaters, employing carbon felt anodes, stainless-steel wool and Ni-foam cathodes, and anion exchange membranes between the electrodes [10–12]. The pilot plant successfully produced high-purity hydrogen (>95 %) continuously over several months, achieving volumetric hydrogen production rates ranging from 0.03 to 0.21 m^3 m^{-3} d^{-1} under controlled conditions of ΔV (0.6–1.4 V) and HRT (1.1–3.9 d).

Currently, several reviews have summarized the substrates, materials, and operational modes of the few pilot-scale MEC studies tested up to date, providing valuable insights into the factors influencing the typically reported poor MEC performance [8,13–15]. In essence, the key bottlenecks detected are the need for optimal reactor configurations to maximize the organic removal rate (ORR), the enhancement of mass transfer rates and electrode materials for boosting current density, the improvement of the energy efficiency of the process, and the development of cost-effective materials. Once these limitations are addressed, MEC technology could provide a sustainable and energy-efficient approach to wastewater treatment and valuable resource recovery. The widespread adoption of MECs is highly dependent on a deep understanding of the critical factors influencing its performance under full-scale conditions. Addressing these factors will enable the development of practical, scalable, and economically viable MEC systems.

With this view, the objective of this study was to design, build, and operate a 1 m^3 MEC pilot plant in a real wastewater treatment plant (WWTP) to evaluate the performance of MEC technology for urban wastewater (UWW) treatment and H_2 production at large scale. The main engineering goal was to assess whether the performance reported in our previous pilot-scale experiences with urban wastewater [10,11] could be achieved in a real scenario using a scaled-up version of the cassette-type prototype. The 1 m^3 MEC was studied for more than 250 days under different operational conditions, including a preliminary evaluation of the novel cassette configuration and a stepwise integration with the actual wastewater stream. To the best of our knowledge, this study shows the largest double-chamber MEC pilot plant built so far in terms of anodic volume, representing a significant step forward in the scale-up of this technology. Using the experimental long-term results, a preliminary techno-economic analysis of MEC technology was performed to assess its commercial potential. Three key factors were discussed: (i) the revenue generated from H_2 production, (ii) the costs associated with external electricity consumption, and (iii) the capital expenditure (CAPEX) required to construct and implement the MEC.

2. Materials and methods

2.1. 1 m^3 MEC design

The pilot plant (Fig. 1) was based on the cassette-style configuration originally proposed by Heidrich et al. [16,17]. The novel prototype included several modifications based on the previous know-how of the group in the scale-up of MECs [10,11]. A thorough description of the fundamentals of the MEC design can be found in the supplementary information (section S1): detailed calculations of reactor dimensions, electrode specifications, hydraulics, and electrical systems.

The reactor consisted of a rectangular stainless-steel (SS) tank capable of accommodating up to fifteen cassettes, each working as a double-chamber MEC (Fig. 1, S1-S3). The modules were strategically positioned on alternating sides of the reactor with the intention to facilitate an S-type flow and to avoid dead zones. The effective anodic volume was 1 m^3 after placing the fifteen cassette modules inside the tank. The cassettes were made of a central PVC frame of 50 × 114 x (2.5 or 1.5) cm acting as cathode, and two outer PVC frames of 50 × 114 × 0.5 cm (with two 38 × 48 cm windows) holding the anodes. Each anodic window was divided and supported by an X-bracing frame to prevent membrane and electrode deformations due to water pressure and to

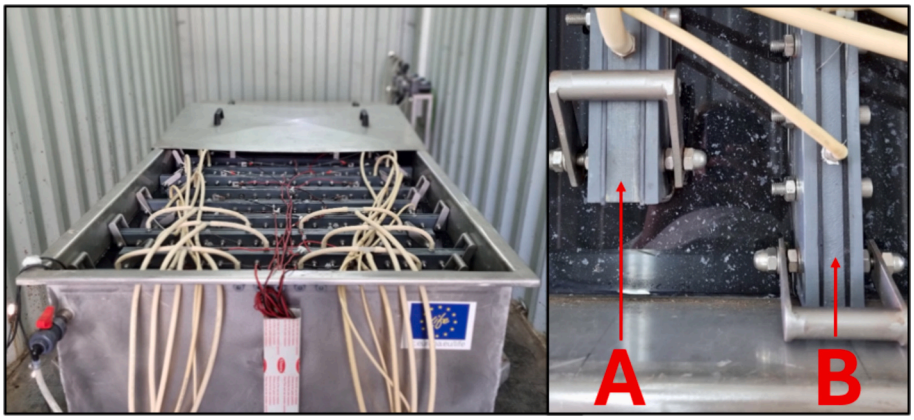

Fig. 1. Left) Overview of the 1 m^3 MEC pilot plant with cassettes in the WWTP; Right) Comparison of the two cassette configurations studied, A (internal frame thickness of 2.5 cm) and B (internal frame thickness of 1.5 cm).

ensure sealing. Furthermore, two different sizes of internal cathode section were tested: i) Configuration A, with an internal frame thickness of 2.5 cm, and ii) Configuration B, with an internal frame thickness of 1.5 cm (Fig. 1). Each cathode was bounded on each side by an anion exchange membrane (AEM), leaving the corresponding anode on the other side. The total cathodic volume per cell was 9 L in Configuration A and 5.5 L in Configuration B, yielding a projected anode surface area to cathode volume ratio of 80.0 and 133.4 m^2 m^{-3}, respectively. These values represented a 101 % and 236 % increase in this ratio compared to the previous cassette [11], which should result in a decrease of the minimum applied potential (ΔV) to drive the process, and a lower cell volume. On the other hand, the total projected anode surface area of a cell was 0.73 m^2 (0.183 m^2 per window and two windows per side), resulting in a maximum projected anode surface of 10.95 m^2 in the reactor. The anode pair and the cathode were separated with functionalized polystyrene AEMs (RALEX® AMHPP, Mega, Czechia), which was selected based on availability, durability under long-term operation, compatibility with wastewater conditions, and ease of integration into the modular system due to its mechanical strength. The anodes were composed of carbon felt (PX35 Carbon Felt, Zoltek™, United States) and were tightly pressed to the AEMs on both sides of the cathode employing a SS mesh. A titanium wire (0.8 mm diameter) was wound into the SS mesh for the electrical connections. The cathodes were made of nickel (Ni) foam (RCM-Ni4753, Recemat BV, The Netherlands) or SS-wool (Steel wool #2, Barlesa SL, Spain), two materials which were successfully employed in the previous prototype [12]. Each cathodic chamber had a pair of gas collection ports located on the top of the central frame to facilitate the gas extraction through a tubing line (Marprene® Tubing 9.6 mm BORE, Watson Marlow, United Kingdom) linked to a 25 L gas sampling bag (FlexFoil® Standard, SKC, United States). Ethylene propylene diene monomer (EPDM) gaskets (2 mm thickness) were employed between the frames to ensure a robust and airtight seal. Fig. 2 shows the different components that collectively form each cassette.

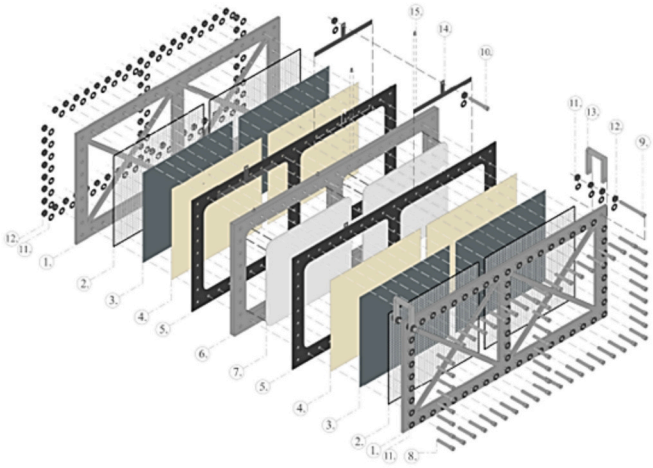

Body part	Description	Material
1	External frame	PVC
2	Anode current collector	SS-316L mesh
3	Anode	Carbon felt
4	Ion exchange membrane	PS AEM
5	Gasket	EPDM
6	Internal frame	PVC
7	Cathode	Ni-foam / SS-304L wool
8	Cassette bolt	SS-316L
9	Shackle bolt	
10	Cathode current collector bolt	
11	Cassette washer	
12	Cassette nut	
13	Hanging shackle	
14	Cathode current collector	
15	Gas collector	

Fig. 2. Exploded view of the novel MEC cassette prototype.

2.2. MEC pilot plant operation

2.2.1. Operation of a cassette with synthetic wastewater (SWW)

The first experimental trial was carried out in the laboratory using a single cassette (Configuration A; Ni-foam cathode). This cell was integrated into the previous L-scale pilot plant (Fig. S6), resulting in most of the tank being the anodic chamber, with an anodic working volume of 193 L. To align with the inoculation strategy planned for the subsequent 1 m^3 pilot-scale MEC, the cassette was started-up in continuous mode with hydraulic retention time (HRT) = 2 d. Acetate was used as sole carbon source, organic loading rate (OLR) was 0.50 g COD L^{-1} d^{-1} and applied voltage ΔV = 1.0 V. The inoculum was anaerobic sludge from the same WWTP of El Prat de Llobregat (Barcelona, Spain). It was added to the anodic feeding tank to achieve a concentration of volatile suspended solids (VSS) of 1.5 g L^{-1}. An internal recycle of 200 L d^{-1} was used to improve turbulence in the reactor (i.e. decrease external mass transfer resistance near the biofilm). After inoculation, the effect of the ΔV on performance was studied. ΔV was gradually reduced from 1.40 V to 0.40 V, at 0.10 V intervals. This range was selected to prevent the cell from experiencing excessively high or low potentials, as these could cause irreversible damage to the biofilm. H_2 production was measured twice at each ΔV, with intervals set to accumulate sufficient gas for

reliable quantification and applied uniformly for all ΔV.

Both the influent and internal recycle flows were established using two timed peristaltic pumps (520 FAM/R2, Watson Marlow, United Kingdom). The feeding solution was prepared with demineralized water with no extra addition of buffer or nutrients solution and stored in a 120 L tank. A 4 g L^{-1} NaCl solution was used as the catholyte due to its low cost, adequate conductivity, and proven stability in previous MEC studies, while also minimizing the risk of biological contamination and precipitation under alkaline conditions. The catholyte was not recycled nor renewed throughout the experiment, and its pH was monitored weekly.

2.2.2. Operation of the pilot plant with real urban wastewater

The second experimental trial was carried out onsite at the WWTP to evaluate the actual performance of the MEC under real operational conditions.

2.2.2.1. Stage I. In stage I, three cassettes (Configuration A) were integrated into the 1380 L SS tank of the pilot plant (Fig. S7), resulting in an anodic working volume of 1310 L. The cathodes used were Ni-foam for cassettes 1–2 and SS-wool for cassette 3. The cassettes were inoculated with urban wastewater in continuous mode and started-up at ΔV = 1.0 V, HRT = 1 d and an OLR ranging between 0.31 and 0.69 g COD L^{-1} d^{-1}, with an internal recycle of 2000 L d^{-1}. In this case, the initial concentration of VSS in the anolyte ranged between 0.08 and 0.32 g L^{-1} due to the inherent variability of the UWW composition. Throughout the entire experiment, real wastewater was directly fed from the main collector at the outlet of the primary settlers without any amendment, except for the addition of one pulse of acetate (~1.5 kg; final COD concentration = 1415 mg L^{-1}) performed at day 80 to investigate the maximum exoelectrogenic activity of the MEC without substrate limitation. The average wastewater composition during Stage I is shown in Table 1. The influent stream was equipped with a prefilter (FD246, Ferdom, Poland) to remove large particles that may have not been removed during primary treatment. Influent, effluent, and internal recycle flows were controlled using three timed peristaltic pumps (520 FAM/R2, Watson Marlow, United Kingdom). The same catholyte of 4 g L^{-1} NaCl solution was used, and its pH was measured every two weeks.

2.2.2.2. Stage II. In a second stage, the capacity of the pilot plant was increased to ten cells resulting in an anodic working volume of 1168 L (Fig. 1). In this case, all cells were assembled with Ni-foam cathodes, and both cell configurations A and B were studied under different conditions for over 100 days. The previous start-up strategy was followed and the MEC was inoculated under the same operational conditions as described in the previous section. After inoculation, the plant was operated under continuous mode with UWW at ΔV = 1.0 V, under two different HRTs: 1 and 2 d. The average wastewater composition during Stage II is shown in Table 1.

2.3. Applied potential and current monitoring

Voltage was supplied by programmable DC power sources (LABPS3005DN, Velleman Group, Belgium). The electrodes were connected to the power sources through 1.5 mm^2 section insulated copper wires and SS connection strips. Current and voltage were digitally monitored with the AddControl software programmed in NI LabWindows CVI [18]. Current intensity and applied voltage were logged every 5 min.

Table 1
Average characteristics of 30 samples of urban wastewater collected during each experimental stage.

Parameter	Stage I	Stage II
COD (mg L^{-1})	509 ± 144	352 ± 105
COD_S (mg L^{-1})	371 ± 103	253 ± 87
Total N (mg L^{-1})	76 ± 6	64 ± 14
P-PO_4^{3-} (mg L^{-1})	7 ± 3	8 ± 2
Total suspended solids (mg L^{-1})	187 ± 97	115 ± 59
Conductivity σ (mS cm^{-1})	2.7 ± 0.2	2.7 ± 0.3
pH	7.5 ± 0.1	7.7 ± 0.1

2.4. Analytical methods

Liquid samples withdrawn from the anode chamber were first passed through 0.22 μm pore-size membrane filters prior to analysis. Organic matter content was determined via COD kits (Hach, LCK 514, USA), using a spectrophotometer (Hach DR2800). Total N was quantified by high temperature catalytic combustion with a multi N/C® 2100S TOC/TNb analyzer (Analytik Jena, Germany). Phosphate concentration was measured using a phosphate analyser (PHOSPHAXsc, Hach Lange), which applies the vanadomolybdate yellow colorimetric method.

Gas from the cathode chamber was characterised by gas chromatography (Agilent Technologies, 7820-A), fitted with two columns: a packed column Porapak Q 80/100 3 ft. G3591–81136 (1.38 m ± 2 mm) and a molecular column MolSieve 5 A 80/100 3 ft. G3591–80017 (1.83 m ± 2 mm), from Agilent Technologies. H_2 and methane production were quantified following the Gas Bag Method described by Ambler and Logan [19]. Methodological details are available in the supplementary information (section S2).

Anodic temperature (Pt1000 thermoresistance, Axiomatic, Spain), pH (HACH Crison5335), and conductivity (HACH Crison5388) were monitored online and logged using the AddControl software.

2.5. Key performance indicators (KPIs)

Current density (*j*) was calculated as current normalized by projected anode area (A m^{-2}). H_2 production was reported per anode area (L m^{-2} d^{-1}) and per anodic volume (m^3 m^{-3} d^{-1}). Cathodic gas recovery (r_{CAT}) compared electrons in H_2 to electrons reaching the cathode. Coulombic efficiency (CE) compared coulombs recovered as current to the theoretical from substrate oxidation. Energy production (E_P) was the energy in H_2; energy consumption (E_C) was the electrical input; energy recovery (r_E) = E_P/E_C. Calculations followed our previous work [11]; details are provided in SI (S3).

2.6. Preliminary techno-economic assessment

The profitability of the pilot plant was evaluated through the methodology proposed by [8]. Profitability was defined as the ratio of H_2 revenue (€) to electricity cost (€), as shown in Eq. 1. The equation was further developed to isolate two different terms; one exclusively related to the MEC performance (H_2 production per kWh electricity (kg H_2 kWh^{-1})) and the other associated with the market prices (the H_2 selling price (€ kg^{-1} H_2) and electricity price (€ kWh^{-1})):

$$\text{Profitability} = \frac{\text{Revenue from hydrogen}}{\text{Electricity cost}} = \frac{\text{H}_2\text{ production}}{\text{Electricity consumption}} \cdot \frac{\text{H}_2\text{ selling price}}{\text{Electricity price}} \quad (1)$$

The first term was calculated with Eq. (2) based on the operational performance of the MEC.

$$\frac{\text{H}_2\text{ production}}{\text{Electricity consumption}}\left(\frac{\text{kg H}_2}{\text{kWh}}\right) = \frac{\frac{r_{CAT}\cdot\int_{t_0}^{t_f} I\,dt}{b_{H_2}\cdot F}\cdot\frac{M_{H_2}}{1000}}{\int_{t_0}^{t_f} I\cdot\Delta V\,dt\cdot\frac{1h}{3600s}\cdot\frac{1kWh}{1000VAh}} = \frac{1}{26.8}\cdot\frac{r_{CAT}}{\Delta V} \quad (2)$$

The second term was defined as the price ratio (PR) with Eq. (3).

$$PR\left(\frac{\text{kWh}}{\text{kg H}_2}\right) = \frac{\text{H}_2\text{ selling price}}{\text{Electricity price}} \quad (3)$$

Combining these terms, the profitability (dimensionless) was ultimately calculated through eq. (4):

$$\text{Profitability} = \frac{1}{26.8}\cdot\frac{r_{CAT}}{\Delta V}\cdot PR \tag{4}$$

The treatment cost was calculated based on Eq. (5). Similar to the profitability, the equation was reformulated to isolate two different terms, one exclusively related to the MEC performance (kWh consumed per kg COD removed) and the other associated with the electricity price (€/kWh).

$$\text{Treatment cost}\left(\frac{€}{\text{kg COD}}\right) = \frac{\text{Electricity cost}}{\text{Treatment capacity}} = \frac{\text{kWh}}{\text{kg COD}}\cdot\text{Electricity price} \tag{5}$$

The first term of Eq. (5) was calculated based on the operational performance of the MEC (Eq. (6)):

$$\frac{\text{kWh}}{\text{kg COD}} = \frac{CE\cdot\left(\frac{M_{O_2}}{1000}\right)^{-1}\cdot b_S\cdot F}{\int_{t_0}^{t_f} I\,dt}\cdot\int_{t_0}^{t_f} I\cdot\Delta V\,dt\cdot\frac{1h}{3600s}\cdot\frac{1kWh}{1000\,VAh} = 3.35\cdot\Delta V\cdot CE \tag{6}$$

Combining Eqs. (5) and (6), the treatment cost was ultimately calculated through Eq. (7):

$$\text{Treatment cost} = 3.35\cdot\Delta V\cdot CE\cdot\text{Electricity price} \tag{7}$$

The net present value (NPV) (Eq. (8)) was employed to evaluate the economic viability over a hypothetical twenty-year operational lifespan, including a one-year construction phase.

$$NPV = \sum_{t=0}^{n}\frac{C_t}{(1+r)^t} \tag{8}$$

with t = Time period; Ct = Cash flow in period t; and r = Discount rate

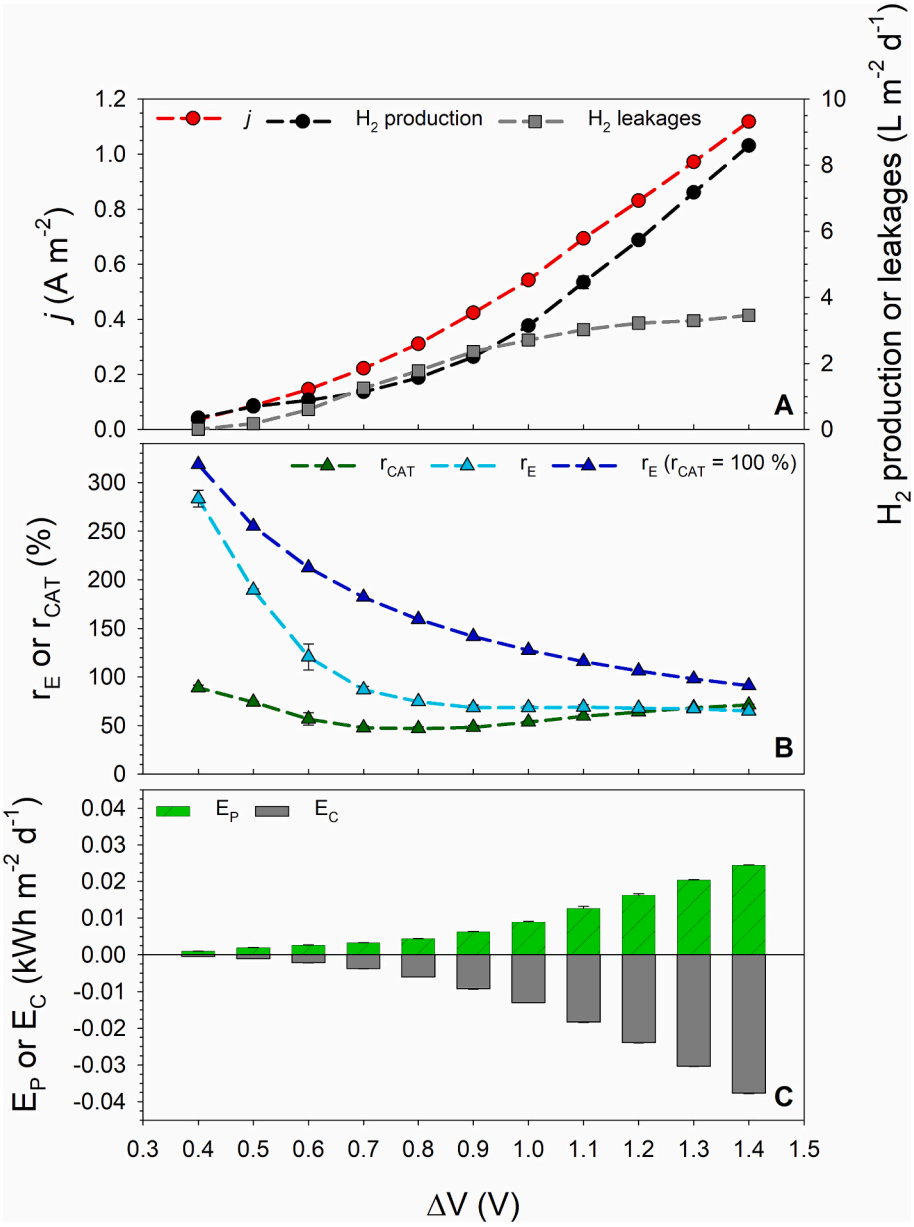

Fig. 3. Key performance indices of a cassette MEC fed with SWW under different ΔV. A) Current density (*j*), specific hydrogen production rate and estimated hydrogen leakages. B) Cathodic recovery (r_{CAT}), experimental energy recovery (r_E) and theoretical energy recovery (assuming r_{CAT} = 100 %). C) Energy production (E_P) and energy consumption (E_C).

(%).

The cash flows represent the net income generated by the system after deducting operating expenses and any additional expenses incurred. These cash flows were estimated considering the initial investment of the pilot plant, the electricity costs and the H_2 selling revenue. On the other hand, the discount rate represents the investor's minimum acceptable rate of return, also known as the cost of capital. This rate reflects the opportunity cost of investing in the project versus other available options. The discount rate (r) was assumed to be equal to that of the Spanish government, at 2 % [20].

3. Results and discussion

3.1. Performance of a single cassette fed with synthetic wastewater

A first experiment using a single cassette (Configuration A) was conducted in a 193 L tank under controlled conditions and SWW (acetate as sole carbon source at $\Delta V = 1.0$ V, HRT = 2 d and OLR = 0.50 g COD L^{-1} d^{-1}). The maximum current density during inoculation was 0.74 A m^{-2}, and the specific H_2 production rate was 5.03 L H_2 m^{-2} d^{-1}. Inoculation was finished at day ~13 when stable performance over time was observed (Fig. S8). Afterwards, different ΔVs were tested maintaining the same hydraulic conditions and temperature to understand its effect on the plant performance (Fig. 3), and to decide the most suitable voltage to be applied in the 1 m^3 pilot plant. The obtained profiles show that higher ΔVs lead to higher current densities and H_2 production rates. The minimum ΔV requirement to drive the hydrogen evolution reaction (HER) was 0.40 V, yielding 0.35 ± 0.01 L H_2 m^{-2} d^{-1} and 0.04 ± 0.01 A m^{-2}. Even though H_2 production was relatively low at this ΔV, it was demonstrated that H_2 can be produced at pilot-scale under low ΔV, which sets a minimum threshold when improving the process efficiency. On the other hand, the maximum specific H_2 production rate was observed at the highest ΔV tested (1.4 V): 8.59 ± 0.06 L H_2 m^{-2} d^{-1}. Assuming full operation of the pilot plant with 15 cassettes (S/V = 10.95 m^2 m^{-3}), the MEC could potentially generate up to 0.094 m^3 H_2 m^{-3} d^{-1}. Furthermore, the high r_E (r_E > 200 %) observed at low ΔV (Fig. 3B) underscores the potential for efficient hydrogen production, showing that the gas generated contained twice the energy required to drive the process. r_E values exceeding 100 % indicate that more energy is recovered as H_2 than is supplied by the electrical input. This reflects the additional energy provided by the microbial oxidation of organic matter in the anode chamber. When the applied voltage is relatively low, this microbial contribution is significant, leading to r_E values greater than 100 %. However, r_E decreases as the ΔV increases until 0.9 V, where r_E reaches a plateau around 67 ± 2 %, mostly due to an increase in E_C (Fig. 3C). Therefore, the optimal ΔV under these conditions was found to be in the range 0.6–0.7 V: a reasonable H_2 production can be obtained (~1.00 L H_2 m^{-2} d^{-1}) without sacrificing the energy efficiency of the process (~100 %).

H_2 losses were also significantly influenced by the ΔV. The initial region of the curve (low ΔV) followed a linear relation, whereas the high ΔV region was not significantly affected (Fig. 3A), causing r_{CAT} to decrease with ΔV until its lowest value at $\Delta V = 0.8$ V (r_{CAT} = 47 %, Fig. 3B). H_2 losses in MECs can arise from multiple pathways. In single-chamber configurations, biological consumption processes (commonly through acetogenesis and methanogenesis) and physical leakage may occur concurrently, while in double-chamber configurations the range of biological cathodic H_2 consumption mechanisms is more limited due to the physical separation of the chambers and the high pH conditions. In the present study, the combination of negligible COD levels in the catholyte, sustained high cathodic pH (>12) across all cassettes, and the high H_2 purity of the collected gas (>93 % with <2 % methane), indicates minimal biological H_2 consumption in the cathodic chamber and mostly physical leakages. Hence, the variability of H_2 leakages over time might be attributed to pressure variations in the cathode chamber. Some of the engineering solutions that could be implemented are: i) employing diaphragm seals between the cathode chamber and the H_2 collection system; ii) removing H_2 from the cathode chamber by forced extraction methods like vacuum pumps [21]; or iii) implementing regular maintenance protocols (pressure monitoring systems for leak detection and repair), to address any potential leaks before damage is exacerbated. In fact, if no H_2 losses are assumed (i.e., $r_{CAT} = 100$ %), the MEC would yield significant H_2 production rates with high r_E efficiencies (r_E > 100 %) under a wide range of ΔV, achieving values as high as r_E = 319 % (ΔV = 0.4 V) or 8.96 ± 0.20 L H_2 m^{-2} d^{-1} with r_E = 106 % (ΔV = 1.2 V) (Fig. 3B). These results underscore the importance of addressing gas leakages in MECs at pilot-scale to ensure optimal performance and efficiency.

3.2. Performance evaluation of the pilot plant with urban wastewater

3.2.1. Stage I: three cells on a real environment

In the initial stage, three cells (Configuration A) were operated for over 100 days in the 1 m^3 MEC pilot plant fed with UWW (see Table 2). In this case, the reactor was inoculated under continuous mode with UWW at $\Delta V = 1.0$ V, HRT = 1 d and an OLR between 0.31 and 0.69 g COD L^{-1} d^{-1}. The start-up phase was significantly longer than that observed in the laboratory (Section 3.1) and the cassettes exhibited a lag phase of ~3.0 d and required over 20 days to reach a pseudo steady-state (Fig. S9). The longer acclimation period could be attributed to several factors, including the variability of wastewater properties (e.g., COD content and biodegradability, conductivity, temperature, etc.) and the inoculation strategy (i.e. UWW had lower biomass concentration compared to the anaerobic sludge). Nevertheless, a functional biofilm for MEC directly from real UWW was obtained in a relatively short term without the need of external addition of acetate or a buffer solution to induce exoelectrogenic activity as in many literature reports. The high recirculation ratio and continuous feeding, combined with the inherent characteristics of the cassette design, facilitated the rapid and efficient inoculation of the MEC. Continuous H_2 production was maintained across all cassettes for over 100 days, demonstrating operational robustness and stability (Fig. S9). The gas production rate remained relatively stable throughout the experimental period despite the inherent variations in the wastewater characteristics. The average specific H_2 production rates for cassettes 1–3 were 2.80 ± 0.65 L m^{-2} d^{-1}, 2.25 ± 0.54 L m^{-2} d^{-1}, and 1.77 ± 0.35 L m^{-2} d^{-1}, and the cumulative H_2 productions during the 100 days of operation were 174.3 L, 129.4 L and 100.8 L. Furthermore, the r_{CAT} and r_E values for all cassettes were consistently around 65 ± 3 % and 81 ± 6 %, respectively.

During days 80 to 92 (Figs. S9-S10), the plant was operated in batch mode by increasing the COD concentration up to 1400 mg COD L^{-1} through the addition of concentrated acetate. This phase aimed to simultaneously improve H_2 production, to investigate potential constraints related to the anode/cathode and to understand the balance between fermentative and exoelectrogenic bacteria. A sudden increase in current density and H_2 production was observed in all cassettes, reaching a peak of 0.56 A m^{-2} and 3.96 L m^{-2} d^{-1} in cassette 1. This increase clearly shows that during the operation with UWW exoelectrogens were limited by the availability of a suitable carbon source such as acetate. Nevertheless, reactor performance started to decrease after one week, aligned with COD depletion, with values dropping below 0.15 A m^{-2} (2.00 L H_2 m^{-2} d^{-1}).

The average H_2 production rate during this batch was 2.67 ± 0.77 L m^{-2} d^{-1}, which did not significantly differ from that obtained in continuous operation with UWW (2.19 ± 0.63 L m^{-2} d^{-1}). In any case, the biofilm was adapted to the typical low substrate levels from continuous operation with UWW, establishing a diverse and specific microbial community tailored to those conditions, and with the amount of exoelectrogens that can survive with the available carbon source. In this sense, the biofilm formation during the batch period was limited by the short exposure time to high substrate conditions, as the fast depletion of COD prevented the formation of a stable biofilm enriched in

Table 2
Summary of the most important results obtained during Stage I.

Operational phase (d)	OLR (g COD L^{-1} d^{-1})	ORR (g COD L^{-1} d^{-1})	T (°C)	Ni-foam (MEC 1/2)		SS-wool (MEC 3)	
				j_{max} (A m^{-2})	H_{2max} (L m^{-2} d^{-1})	j_{max} (A m^{-2})	H_{2max} (L m^{-2} d^{-1})
Inoculation t = 0–25	0.43 ± 0.13	0.08 ± 0.03	18 ± 1	0.51 ± 0.05	2.58 ± 1.25	0.28	1.58
Continuous t = 35–80	0.39 ± 0.11	0.09 ± 0.03	19 ± 2	0.45 ± 0.04	3.33 ± 0.72	0.31	2.11
Batch t = 80–92	–	0.14 ± 0.10	23 ± 1	0.53 ± 0.07	3.64 ± 0.45	0.36	2.37
Continuous t = 92–110	0.40 ± 0.06	0.07 ± 0.02	25 ± 2	0.31 ± 0.05	2.13 ± 0.54	0.20	1.83

exoelectrogens, resulting in negligible changes in performance. This is further supported by the low CE observed (6.3 %), which indicates that a large portion of the added acetate was consumed through non-exoelectrogenic pathways.

3.2.2. Stage II: Ten cells on a real environment

The capacity of the pilot plant was increased to ten cells to further evaluate the performance and stability of the MEC. Furthermore, two different sizes of internal cathode section were tested: i) Configuration A, with an internal frame thickness of 2.5 cm; ii) Configuration B, with an internal frame thickness of 1.5 cm (Fig. 1B). The MEC was again inoculated under continuous mode with UWW under the same operational conditions. The inherent presence of exoelectrogenic biomass in the bulk liquid from the previous stage and the higher summer operating temperature (>30 °C) contributed to a faster establishment of an active biofilm.

By day 25 of operation, all cassettes had established stable performance and exhibited continuous H_2 production until the end of Stage II (Fig. 4). The plant was operated under continuous mode with UWW at $\Delta V = 1.0$ V under two different HRTs: 1 and 2 d. The inlet COD_S concentration ranged from 103 to 345 mg L^{-1} (average soluble $COD_I = 253 \pm 87$ mg L^{-1}, OLR = 0.12–0.44 g COD L^{-1} d^{-1}). At HRT = 1 d, the MEC yielded an average total COD removal of 34 ± 5 % and a soluble COD removal of 25 ± 6 %, and increased up to 51 ± 4 % and 45 ± 2 % when operating at HRT = 2 d (Fig. 5). Furthermore, CE was boosted, yielding an average efficiency of 31 ± 7 % and 28 ± 4 %, at an HRT of 1 and 2 d, respectively. These results agree with the CEs typically reported at pilot-scale (>30 %, [15]), but still far from the reported at lab-scale with acetate (>70 %, [22]), which indicates the effect of a more complex scenario. Further reactor optimization would be required to favour exoelectrogenic activity over other biological processes, ultimately leading to enhanced CEs.

In contrast to COD removal efficiencies, no significant variations in H_2 production rates were observed under the HRTs tested. The average volumetric H_2 production rate remained relatively stable at 0.015 ± 0.005 m^3 H_2 m^{-3} d^{-1}, with a peak production of 0.021 m^3 H_2 m^{-3} d^{-1} (Fig. 4). This may be attributed to the influence of the varying temperature in the anolyte or to the limited COD concentration in the reactor, masking the effect of the HRT in performance. The average r_{CAT} and r_E were also stable throughout Stage II, consistently maintaining values around 65 % and 80 %, respectively (Fig. S12). The highest r_E (90 %) was observed in the cassettes with Configuration B, demonstrating the benefits of this configuration for enhanced r_E.

Fig. 6 compares the performance of Configurations A and B during the continuous operation of the pilot plant. Configuration B exhibited the best performance during the whole operation, yielding an average current density and H_2 production of 0.39 ± 0.04 A m^{-2} and 2.69 ± 0.35 L H_2 m^{-2} d^{-1}. This represents a 57 % and 53 % increase in current density and H_2 production compared to Configuration A. These improved results were mainly attributed to the shorter inter-electrode distance, which led to a decrease in the cell overpotential. Considering the possible operation of the pilot plant with 15 cassettes under configuration B (i.e. S/V = 10.95 m^2 m^{-3}), the maximum current density and H_2 production (i.e. 7.29 L m^{-2} d^{-1}), the reactor could potentially generate up to 0.042 m^3 H_2 m^{-3} d^{-1} (Fig. 4).

These results are promising given the typical H_2 production rates

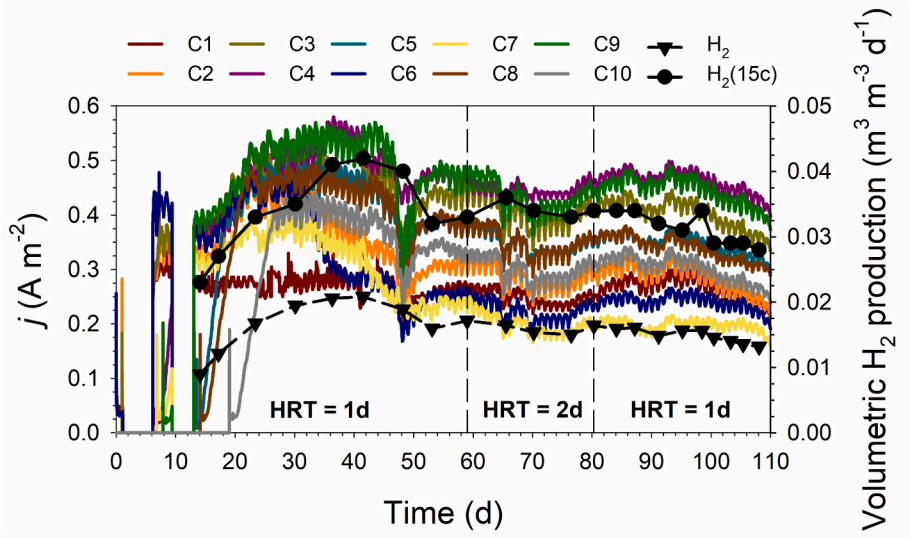

Fig. 4. Current density (*j*) and volumetric hydrogen production rate (H_2) during the continuous operation of the pilot plant (10 cassettes) with real wastewater. H_2(15c) refers to the estimated volumetric hydrogen production rate considering 15 cassettes yielding the maximum performance obtained.

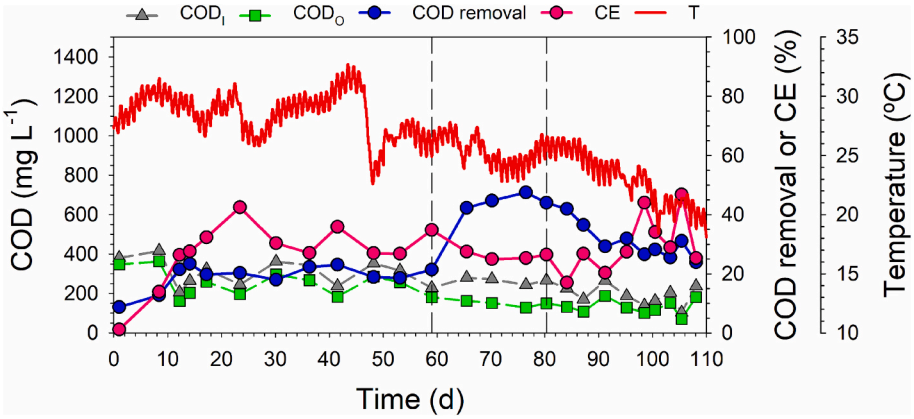

Fig. 5. Continuous operation of the pilot plant (Stage II, 10 cassettes) with real wastewater. Inlet soluble COD concentration (COD_I), outlet soluble COD concentration (COD_O), coulombic efficiency (CE), soluble COD removal efficiency (COD removal) and temperature profile of the reactor. Dashed lines indicate the start and end time of the continuous operation at HRT of 2 d.

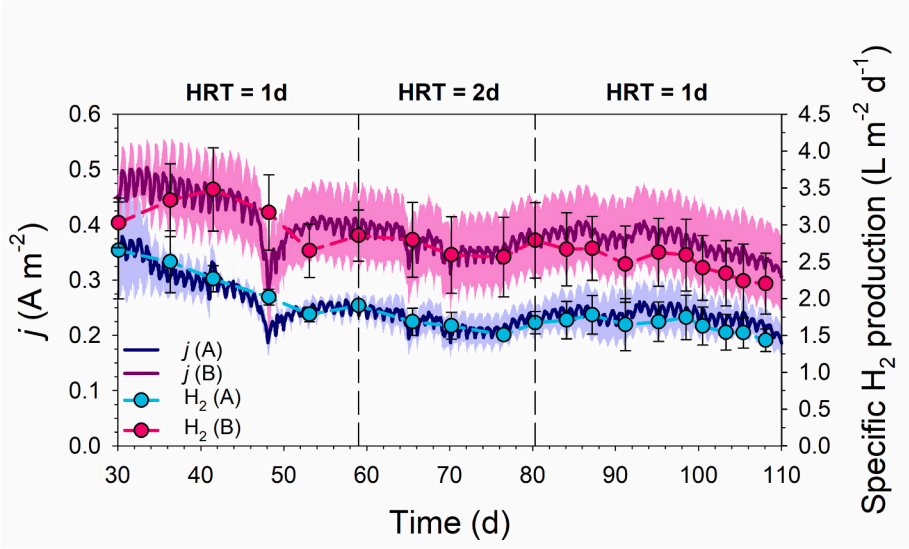

Fig. 6. Comparison of the current density (j) and specific hydrogen production rate (H_2), during the continuous operation of the pilot plant (10 cassettes) with urban wastewater, between Configuration A and B. Shades indicate standard deviation of current density.

reported in MEC pilot reactors fed with real wastewater (>100 L). A summary of key performance parameters from previous cassette-type MEC pilots and the present work is provided in Table S3 (SI), for direct comparison. The first MEC pilot plant was the 1 m^3 single-chamber reactor proposed by Cusick et al. [9], which was operated for 100 days with winery wastewater but, over the long term, methanogenesis became dominant and the H_2 produced was biologically consumed. Methanogenesis inhibition/mitigation/suppression has been addressed in subsequent MEC pilot plant prototypes by adopting a double-chamber configuration in different reactor architectures [8]. However, only litre-scale reactors have yielded high H_2 production rates using real wastewater (>1 m^3 m^{-3} d^{-1}), with reactors larger than 10 L typically producing significantly lower values (>0.1 m^3 m^{-3} d^{-1}). The highest H_2 production rate reported in a semi pilot-scale MEC (V_{anode} = 10 L) up to date was 0.71 m^3 m^{-3} d^{-1}, using lignocellulosic hydrolysate as a substrate [23]. In double-chamber MECs with anodic volumes larger than 100 L treating UWW, performance further diminishes, and H_2 production rates typically range from 0.005 to 0.038 m^3 H_2 m^{-3} d^{-1} [11,24]. Therefore, the results obtained in the present study address some of the technical challenges associated with large-scale MEC reactors as the performance of the 1 m^3 prototype was comparable to that of the previous 135 L MEC. As suggested by previous authors [24,25], the efforts should now be directed toward bridging the gap between millilitre and litre scale performance, minimizing H_2 leakages and decreasing the internal resistance of the whole system. Furthermore, the inherent low-COD strength of UWW is the primary cause of the low current densities (and H_2 production rates) usually reported. New MEC designs, such as the one proposed by Jiang et al. [26] for a high COD strength industrial effluent, may help to improve performance, although it has not yet been demonstrated whether improvement would be possible when treating low COD strength urban effluents with low conductivity. Therefore, MEC technology should find a better niche in high-strength (industrial) wastewater streams, where its benefits are most pronounced.

3.3. *Preliminary techno-economic assessment of the MEC*

Assessing the techno-economic viability of MECs is crucial for understanding their market potential. Even if market adoption seems distant, this techno-economic assessment helps to identify potential technical and economic hurdles early on. This allows for adjustments to the technology or business model, ensuring that it remains viable and competitive. Currently, only few studies have addressed this aspect [8,13,27,28]. The techno-economic assessment of this work is

intentionally device-level, focusing on applied electrical energy to the MEC stack and capital costs; auxiliary balance-of-plant loads (e.g., influent/recirculation pumping, gas handling, controls) are excluded from the base case due to their strong site- and layout-specific dependence and can be incorporated in a future plant-level assessment.

3.3.1. Profitability

Based on the H_2 sales revenue and the electricity consumption costs, profitability (Eq. (4)) was calculated for the different MEC performance scenarios reported in Table 3 (Fig. 7). Considering the current average electricity cost for the industrial sector in Spain (0.1 € kWh^{-1} [29]) and the selling price range of green H_2 in the EU: 4–8 € kg^{-1} H_2 [30], the PR would range from 40 kWh kg^{-1} H_2 (at the minimum selling price) to 80 kWh kg^{-1} H_2 (at the highest selling price). At a PR of 40 kWh kg^{-1} H_2, the operation of the pilot plant becomes profitable only in the case of SWW with low ΔV and high r_{CAT} (Case 4). Under these conditions, profitability was 3.3, i.e., the revenue from the sale of H_2 would be 3.3 times the cost of electricity. In contrast, the operation with UWW (Case 1) would not be profitable due to the relatively low r_{CAT} attained and high ΔV required. This economic inefficiency is not directly correlated to the H_2 production rate. For instance, the performance with UWW (Case 1) and SWW at ΔV of 1.0 V (Case 5) or 1.4 V (Case 6), revealed significantly different H_2 yields while maintaining similar profitability. Nonetheless, considering a PR of 80 kWh kg^{-1} H_2, all cases become profitable.

These results clearly indicate that MEC should be operated at low ΔV with minimal H_2 losses to reduce the dependence on external electricity and hydrogen sales prices for profitability. While achieving r_{CAT} close to 100 % in double-chamber systems seems to be an exclusively technical/engineering challenge, and therefore achievable, obtaining significant H_2 production by applying a low ΔV (i.e. close to the theoretical potential value, 0.123 V) is practically unattainable due to the intrinsic properties of UWW and the voltage losses observed in the reactor. However, a substantial reduction in the ΔV is feasible by improving the reactor design, addressing technical aspects such optimizing flow distribution or module configuration (number and size of stacks, electrode spacing, materials, electrical connections, etc.), and/or using high-strength or high-conductive wastewaters. With this view, the most suitable wastewater streams would be those derived from food, beverage, alcohol or biofuel processing, and other similar industries [31].

In an ideal scenario, where the theoretical potential (ΔV = 0.123 V) is enough to drive HER and no H_2 losses occur (r_{CAT} = 100 %), the PR limit would be very low (3.30 kWh kg^{-1} H_2, Table 3), and the MEC could potentially generate 25 times more revenue from H_2 sales than electricity costs if the H_2 selling price was maximum (8 € kg^{-1} H_2). This favourable economic outlook would ensure the profitability of the MEC across a wide range of PR values, thereby significantly reducing the investment risk associated with its implementation.

Table 3
Description of the different cases evaluated to assess profitability in the 1 m^3 MEC pilot plant. PR limit refers to the lowest price ratio threshold for a profitability of 1.

Case	Description	PR limit (kWh kg^{-1} H_2)
1	Average performance with UWW (r_{CAT} = 65 %; ΔV = 1.0 V)	41.23
2	Theoretical performance with acetate (r_{CAT} = 100 %; ΔV = 0.123 V)	3.30
3	Theoretical performance with acetate (r_{CAT} = 65 %; ΔV = 0.123 V)	5.07
4	Average performance with acetate (r_{CAT} = 89 %; ΔV = 0.4 V)	12.04
5	Average performance with acetate (r_{CAT} = 54 %; ΔV = 1.0 V)	49.63
6	Average performance with acetate (r_{CAT} = 71 %; ΔV = 1.4 V)	52.85

3.3.2. Wastewater treatment cost

Fig. 8 presents a comparative analysis of the wastewater treatment cost using the MEC pilot plant under four different performance cases (Table 4). The results obtained highlight the pivotal role of both CE and ΔV in determining the treatment cost of the MEC technology. Considering the theoretical performance with acetate (Case C), a remarkable 3.7-fold reduction in the treatment cost was obtained when compared to the conventional activated sludge process (CAS). Furthermore, 3.75 kWh kg^{-1} COD would be produced under these conditions (considering 33 kWh kg^{-1} H_2, [32]). The wastewater treatment cost considering the current performance of the pilot plant with UWW (Case A) would still yield a 2.5-fold decrease in electricity consumption per kg COD removed compared to the reference CAS, as a substantial portion of the organic matter removed is not consumed by the exoelectrogenic bacteria (CE = 31 %), resulting in lower current density and reduced power consumption. If CE was improved, the current density would increase to treat all the input organic matter under the same ΔV, leading to higher treatment costs when compared to the reference CAS. However, more H_2 would be generated and, specifically, the net balance would not be affected. As high CE are generally desired, the only viable operational strategy to reduce the wastewater treatment costs of MECs lies in minimizing the ΔV.

3.3.3. Cost analysis

For the present 1 m^3 MEC pilot plant, material costs accounted for 44,123 €, which were considerably higher than the material costs per unit flowrate (<3000 €/(m^3 d^{-1}) estimated by Aiken et al. [28]. This increase is mainly related to the high costs of manufacturing the cassettes. Specifically, the cassette bodies constituted the greatest proportion of the material costs (49 %), followed by the control system and instrumentation (23 %), and the electrodes and membranes (13 %) (Fig. S13). These components accounted for 85 % of construction costs of the pilot plant.

On the other hand, the NPV was employed to evaluate the economic viability of different scenarios of the pilot plant over a hypothetical twenty-year operational lifespan, including a one-year construction phase. These scenarios ranged from practical to theoretical performance, considering various factors that impact the economic performance of MECs, including H_2 production rate and its revenue, r_{CAT}, ΔV, maintenance costs, and capital expenses (Table S4). Considering a H_2 selling price of 4 € kg^{-1} and the average performance levels observed in the pilot plant with UWW, the NPV was −44,132.09 €. Even with the pilot plant operating at the theoretical potential, yielding a high H_2 production of 1 m^3 m^{-3} d^{-1} and a r_{CAT} = 100 %, the NPV did not vary significantly (−42,745.25 €). Furthermore, those scenarios did not include the impact of maintenance costs. Some components such as the membranes or the electrical connections should require regular maintenance to ensure optimal performance and prevent system failures. For instance, considering an annual replacement of the membranes and the electrical connections, the NPV would decrease down to −72,166.56 €. The NPV could be improved with a significant reduction of the construction costs, as the material costs accounted for 99 % of the NPV. Therefore, electricity cost and the H_2 selling revenue are negligible in most of the cases.

3.4. Future perspectives

MEC technology stands for a sustainable and eco-friendly option for wastewater treatment and H_2 production. Extensive lab-scale research has demonstrated that MECs can achieve energy neutrality or even net energy production, whereas CAS systems typically consume around 0.2 kWh m^{-3} for aeration [33]. However, the techno-economic analysis revealed that material costs pose a major hurdle in a future MEC industrial adoption. The capital expenses reported for CAS are in the range

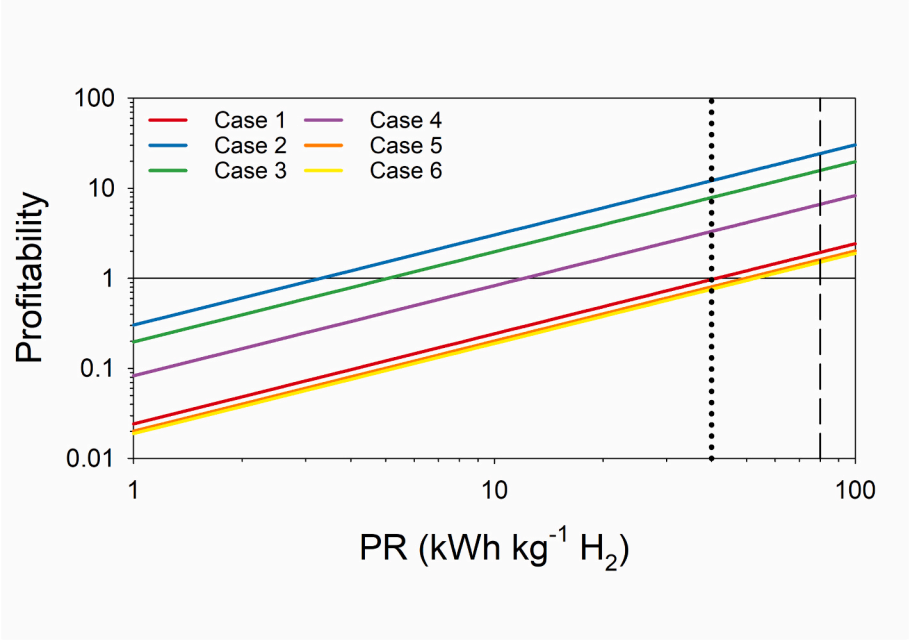

Fig. 7. Profitability of the 1 m^3 MEC pilot plant at different price ratios (PR) and different performance cases (see Table 3 for case descriptions, operational parameters, and PR limits). Black dashed line indicates the PR yielded by the current price of electricity and the EU's hydrogen target price for 2030. Black dotted line indicates the PR yielded by the current prices of electricity and hydrogen.

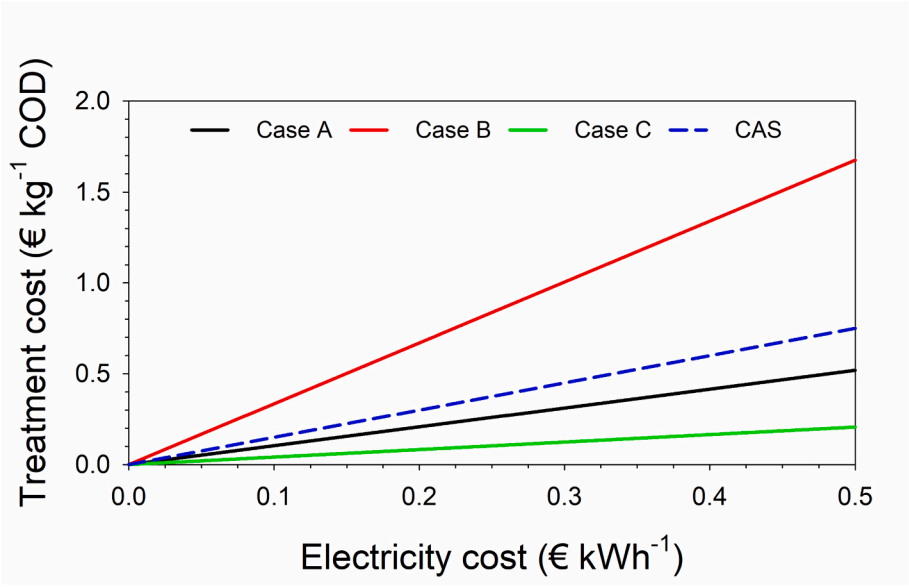

Fig. 8. Treatment cost of the 1 m^3 MEC pilot plant at different electricity prices, for different performance cases (see Table 4 for case descriptions, operational parameters, and associated energy balances). CAS refers to the treatment cost of a reference conventional activated sludge.

of 350–4290 € m^{-3} d^{-1} [34] due to the higher volumetric treatment capacities achieved. These values are two orders of magnitude lower than those in MECs. Even in the best scenario, the NPV remains negative because the revenue from H_2 production is negligible when compared to the high capital expenses. The high CAPEX required hinders its commercial adoption, pointing to the need for research efforts to focus on developing and implementing cost-effective materials for MEC components, prioritizing affordability over maximizing performance at any cost. It includes exploring alternative materials for cassette bodies, optimizing electrode and membrane fabrication techniques, and employing innovative materials that can enhance performance while reducing costs. Furthermore, the long-term durability of materials is a critical aspect impacting their commercial viability, yet poorly understood, which limits the identification of the optimal materials for large-scale applications. For instance, electrode degradation or membrane fouling can also be major issues in MECs [35], which would reduce its efficiency and increase maintenance costs. Developing anti-fouling strategies or preventive electrode deterioration techniques would open new avenues for designing robust and efficient MECs. Standardizing MEC designs and adopting efficient manufacturing techniques for modularization, using recycled materials, could also significantly reduce production costs.

Regarding the possible bottlenecks for H_2 generation at m^3-scale in this pilot, H_2 production was constrained by: (i) limited anodic electron

Table 4
Description of the different cases evaluated to assess the treatment cost in the 1 m^3 MEC pilot plant, kWh of electricity consumed per kg COD removed, kg of hydrogen produced per kg COD removed, and kWh of electricity produced per kg COD removed.

Case	Description	kWh kg^{-1} COD	kg H_2 kg^{-1} COD	kWh kg^{-1} COD (33 kWh kg^{-1} H_2)
A	Average performance with UWW (CE = 31 %; ΔV = 1.0 V)	1.04	0.03	0.21
B	Improved performance with UWW (CE = 100 %; ΔV = 1.0 V)	3.35	0.08	0.65
C	Theoretical performance with acetate (CE = 100 %; ΔV = 0.123 V)	0.41	0.13	3.75
CAS	Reference conventional activated sludge	1.50	0.00	0.00

transfer under low-COD municipal primary effluent, evidenced by a transient boost after acetate pulsing but a very low CE during that batch (6.3 %); (ii) internal resistance/overpotentials, since shortening the inter-electrode gap (Configuration B vs A) increased current density by ~57 %, H_2 production by ~53 %, and raised r_E up to ~90 %; (iii) electrolyte conductivity and matrix constraints: the composition of urban wastewater cannot be readily improved, and adding salts to raise conductivity is neither cost-effective nor desirable because it increases salinity and the contaminant load in the effluent; accordingly, MECs may be better suited to industrial wastewaters with intrinsically higher conductivity and organic strength; (iv) gas-side losses, with sustained high cathodic pH (>12) and high H_2 purity (>93 %, <2 % CH_4) indicating physical leakage as a persistent sink of recoverable gas. From an operational standpoint, external mass-transfer limitations and comparatively low organic removal rates versus conventional processes imply that MECs for urban wastewater will need integration with downstream secondary treatment, and cassette packing density can restrict modularity and complicate maintenance. Priorities to address these limitations include leak-tight gas handling, further reduction of ohmic losses, improved mass transfer, and maintainable cassette integration during scale-up. Finally, because MECs primarily remove organic matter (and recover energy) rather than nutrients, standalone application to urban wastewater would still require a complementary nutrient-removal step operating without organic matter, such as autotrophic nitrogen removal or chemical P precipitation.

4. Conclusions

A novel 1 m^3 MEC pilot plant fed with SWW yielded significant H_2 production rates under a wide range of ΔV, with higher ΔV leading to higher current densities. Under these conditions, the maximum H_2 production was 8.59 ± 0.06 L H_2 m^{-2} d^{-1} (ΔV = 1.4 V) and the minimum ΔV requirement to drive the HER (0.35 L H_2 m^{-2} d^{-1}) was 0.4 V, demonstrating, for the first time, that H_2 can be produced in a large-scale MEC at a low ΔV. The operation of the MEC pilot plant under real conditions demonstrated the ability to establish functional biofilms directly from UWW, eliminating the need for external carbon sources. Continuous H_2 production was achieved during the long-term operation, demonstrating robust operation and stability, even under temperature variations and changes in influent characteristics. The average total COD removal was 34 ± 5 % and 51 ± 4 % at an HRT of 1 and 2 days, respectively. Considering the operation of the pilot plant at full capacity (S/V = 10.95 m^2 m^{-3}) and the maximum H_2 production obtained (7.29 L m^{-2} d^{-1}), the reactor could potentially generate up to 0.042 m^3 H_2 m^{-3} d^{-1}. These results are comparable to those obtained in smaller pilot plants (<100 L), demonstrating the scalability of the proposed cassette design. Comparing the novel MEC prototype with CAS, a significant reduction in the treatment cost per unit of COD removed might be achieved. Nonetheless, based on the H_2 sales revenue and the electricity consumption costs, the pilot plant could be economically profitable only under very specific conditions. The material costs represented a 99 % of the NPV of the novel MEC prototype, overshadowing the benefits of lower electricity costs and the H_2 revenue. Thus, the high capital expenses associated with MEC components hinder commercial viability, emphasizing the need for cost-effective materials and manufacturing techniques.

CRediT authorship contribution statement

Oscar Guerrero-Sodric: Writing – review & editing, Writing – original draft, Visualization, Methodology, Investigation, Data curation, Conceptualization. **Juan Antonio Baeza:** Writing – review & editing, Visualization, Validation, Supervision, Software, Methodology, Formal analysis, Conceptualization. **Albert Guisasola:** Writing – review & editing, Supervision, Resources, Project administration, Methodology, Funding acquisition, Formal analysis, Conceptualization.

Declaration of competing interest

The authors declare the following financial interests/personal relationships which may be considered as potential competing interests: Albert Guisasola reports financial support was provided by European Union. If there are other authors, they declare that they have no known competing financial interests or personal relationships that could have appeared to influence the work reported in this paper.

Acknowledgements

This work was supported by the LIFE+ NIMBUS project (LIFE19 ENV/ES/000191) (www.life-nimbus.eu). The authors are members of the GENOCOV research group (*Grup de Recerca Consolidat de la Generalitat de Catalunya*, 2021 SGR 515, www.genocov.com). Albert Guisasola acknowledges the funding from the ICREA Academia grant (2025-2029), *Generalitat de Catalunya*. We would like to thank *Aigües de Barcelona* for allowing the installation of the plant at the *El Prat de Llobregat* WWTP and CETAQUA for their help in monitoring the plant.

Appendix A. Supplementary data

Supplementary data to this article can be found online at https://doi.org/10.1016/j.cej.2025.168035.

Data availability

Data will be made available on request.

References

[1] P. Swaminathan, A. Ghosh, G. Sunantha, K. Sivagami, G. Mohanakrishna, S. Aishwarya, S. Shah, A. Sethumadhavan, P. Ranjan, R. Prajapat, A comprehensive review of microbial electrolysis cells: Integrated for wastewater treatment and hydrogen generation, Process Saf. Environ. Prot. 190 (2024) 458–474, https://doi.org/10.1016/j.psep.2024.08.032.
[2] E.S. Heidrich, T.P. Curtis, J. Dolfing, Determination of the internal chemical energy of wastewater, Environ. Sci. Technol. 45 (2011) 827–832, https://doi.org/10.1021/es103058w.
[3] M. Osset-Álvarez, L. Rovira-Alsina, N. Pous, R. Blasco-Gómez, J. Colprim, M. D. Balaguer, S. Puig, Niches for bioelectrochemical systems on the recovery of water, carbon and nitrogen in wastewater treatment plants, Biomass Bioenergy 130 (2019), https://doi.org/10.1016/j.biombioe.2019.105380.
[4] L. Rago, J.A. Baeza, A. Guisasola, Bioelectrochemical hydrogen production with cheese whey as sole substrate, J. Chem. Technol. Biotechnol. 92 (2017) 173–179, https://doi.org/10.1002/jctb.4987.
[5] A. Tenca, R.D. Cusick, A. Schievano, R. Oberti, B.E. Logan, Evaluation of low cost cathode materials for treatment of industrial and food processing wastewater using microbial electrolysis cells, Int. J. Hydrogen Energy 38 (2013) 1859–1865, https://doi.org/10.1016/j.ijhydene.2012.11.103.
[6] Y. Wang, W.Q. Guo, D.F. Xing, J.S. Chang, N.Q. Ren, Hydrogen production using biocathode single-chamber microbial electrolysis cells fed by molasses wastewater

at low temperature, Int. J. Hydrogen Energy (2014) 19369–19375, https://doi.org/10.1016/j.ijhydene.2014.07.071. Elsevier Ltd.
[7] J. Ditzig, H. Liu, B. Logan, Production of hydrogen from domestic wastewater using a bioelectrochemically assisted microbial reactor (BEAMR), Int. J. Hydrogen Energy 32 (2007) 2296–2304, https://doi.org/10.1016/j.ijhydene.2007.02.035.
[8] J. Jiang, J.A. Lopez-Ruiz, Y. Bian, D. Sun, Y. Yan, X. Chen, J. Zhu, H.D. May, Z. J. Ren, Scale-up and techno-economic analysis of microbial electrolysis cells for hydrogen production from wastewater, Water Res. 241 (2023), https://doi.org/10.1016/j.watres.2023.120139.
[9] R.D. Cusick, B. Bryan, D. Parker, M. Merrill, M. Mehanna, P. Kiely, G. Liu, B. E. Logan, Performance of a pilot-scale continuous flow microbial electrolysis cell fed winery wastewater, Appl. Microbiol. Biotechnol. 89 (2011) 2053–2063, https://doi.org/10.1007/s00253-011-3130-9.
[10] J.A. Baeza, À. Martínez-Miró, J. Guerrero, Y. Ruiz, A. Guisasola, Bioelectrochemical hydrogen production from urban wastewater on a pilot scale, J. Power Sources 356 (2017) 500–509, https://doi.org/10.1016/j.jpowsour.2017.02.087.
[11] O. Guerrero-Sodric, J.A. Baeza, A. Guisasola, Exploring key operational factors for improving hydrogen production in a pilot-scale microbial electrolysis cell treating urban wastewater, Chem. Eng. J. 469 (2023) 144001, https://doi.org/10.1016/j.cej.2023.144001.
[12] O. Guerrero-Sodric, J.A. Baeza, A. Guisasola, Enhancing bioelectrochemical hydrogen production from industrial wastewater using Ni-foam cathodes in a microbial electrolysis cell pilot plant, Water Res. 256 (2024) 121616, https://doi.org/10.1016/j.watres.2024.121616.
[13] D.C. Aiken, T.P. Curtis, E.S. Heidrich, The rational design of a financially viable microbial electrolysis cell for domestic wastewater treatment, Front. Chem. Eng. 3 (2021), https://doi.org/10.3389/fceng.2021.796805.
[14] A. Fathima, I.M.S.K. Ilankoon, Y. Zhang, M.N. Chong, Scaling up of dual-chamber microbial electrochemical systems – An appraisal using systems design approach, Sci. Total Environ. 912 (2024), https://doi.org/10.1016/j.scitotenv.2023.169186.
[15] R. Rousseau, L. Etcheverry, E. Roubaud, R. Basséguy, M.L. Délia, A. Bergel, Microbial electrolysis cell (MEC): Strengths, weaknesses and research needs from electrochemical engineering standpoint, Appl. Energy 257 (2020), https://doi.org/10.1016/j.apenergy.2019.113938.
[16] E.S. Heidrich, J. Dolfing, K. Scott, S.R. Edwards, C. Jones, T.P. Curtis, Production of hydrogen from domestic wastewater in a pilot-scale microbial electrolysis cell, Appl. Microbiol. Biotechnol. 97 (2013) 6979–6989, https://doi.org/10.1007/s00253-012-4456-7.
[17] E.S. Heidrich, S.R. Edwards, J. Dolfing, S.E. Cotterill, T.P. Curtis, Performance of a pilot scale microbial electrolysis cell fed on domestic wastewater at ambient temperatures for a 12 month period, Bioresour. Technol. 173 (2014) 87–95, https://doi.org/10.1016/j.biortech.2014.09.083.
[18] J.A. Baeza, Advanced Direct Digital Control (AddControl): lessons learned from 20 years of adding control to lab and pilot scale treatment systems, in: in: 13th IWA Conference on Instrumentation, Control and Automation. ICA 2022, Tsinghua University, Beijing (China), 2022, pp. 13–15.
[19] J.R. Ambler, B.E. Logan, Evaluation of stainless steel cathodes and a bicarbonate buffer for hydrogen production in microbial electrolysis cells using a new method for measuring gas production, Int. J. Hydrogen Energy 36 (2011) 160–166, https://doi.org/10.1016/j.ijhydene.2010.09.044.
[20] Banco de España, Interest rates. https://www.bde.es/webbe/es/estadisticas/temas/tipos-interes.html, 2024. (Accessed 3 April 2024).
[21] H. Feng, L. Huang, M. Wang, Y. Xu, D. Shen, N. Li, T. Chen, K. Guo, An effective method for hydrogen production in a single-chamber microbial electrolysis by negative pressure control, Int. J. Hydrogen Energy 43 (2018) 17556–17561, https://doi.org/10.1016/j.ijhydene.2018.07.197.
[22] A. Guisasola, J.A. Baeza, A. Marone, É. Trably, N. Bernet, Opportunities for Hydrogen Production from Urban/Industrial Wastewater in Bioelectrochemical Systems, in: Microbial Electrochemical Technologies, CRC Press, Boca Raton, 2020, pp. 225–243, https://doi.org/10.1201/9780429487118-15.
[23] L. Wang, F. Long, D. Liang, X. Xiao, H. Liu, Hydrogen production from lignocellulosic hydrolysate in an up-scaled microbial electrolysis cell with stacked bio-electrodes, Bioresour. Technol. 320 (2021), https://doi.org/10.1016/j.biortech.2020.124314.
[24] S.E. Cotterill, J. Dolfing, C. Jones, T.P. Curtis, E.S. Heidrich, Low Temperature Domestic Wastewater Treatment in a Microbial Electrolysis Cell with 1 m2 Anodes: Towards System Scale-Up, Fuel Cells 17 (2017) 584–592, https://doi.org/10.1002/fuce.201700034.
[25] J.J. Fornero, M. Rosenbaum, L.T. Angenent, Electric power generation from municipal, food, and animal wastewaters using microbial fuel cells, Electroanalysis 22 (2010) 832–843, https://doi.org/10.1002/elan.200980011.
[26] J. Jiang, L. Du, B. Si, H.D. Kawale, Z. Wang, S. Summers, J.A. Lopez-Ruiz, S. Li, Y. Zhang, Z.J. Ren, Pilot microbial electrolysis cell closes the hydrogen loop for hydrothermal wet waste conversion to jet fuel, Water Res. 268 (2025) 122644, https://doi.org/10.1016/j.watres.2024.122644.
[27] N. Savla, Suman, S. Pandit, J.P. Verma, A.K. Awasthi, S.S. Sana, R. Prasad, Techno-economical evaluation and life cycle assessment of microbial electrochemical systems: a review, Curr. Res. Green Sustain. Chem. 4 (2021), https://doi.org/10.1016/j.crgsc.2021.100111.
[28] D.C. Aiken, T.P. Curtis, E.S. Heidrich, Avenues to the financial viability of microbial electrolysis cells [MEC] for domestic wastewater treatment and hydrogen production, Int. J. Hydrogen Energy 44 (2019) 2426–2434, https://doi.org/10.1016/j.ijhydene.2018.12.029.
[29] STATISTA, Prices of Electricity for Industry in Spain from 2013 to 2024, 2024 https://www.statista.com/statistics/595813/electricity-industry-price-spain/ (accessed March 8, 2024).
[30] H2V, Average Cost of Green Hydrogen, 2025 https://h2v.eu/analysis/statistics/financing/hydrogen-cost-and-sales-prices/ (accessed August 8, 2025).
[31] T. Hyun Chung, B. Ranjan Dhar, A multi-perspective review on microbial electrochemical technologies for food waste valorization, Bioresour. Technol. 342 (2021), https://doi.org/10.1016/j.biortech.2021.125950.
[32] C. Dolle, N. Neha, C. Coutanceau, Electrochemical hydrogen production from biomass, Curr. Opin. Electrochem. 31 (2022), https://doi.org/10.1016/j.coelec.2021.100841.
[33] C.Y. Shi, Mass Flow and Energy Efficiency of Municipal Wastewater Treatment Plants, IWA Publishing, 2011.
[34] T. Gao, K. Xiao, J. Zhang, W. Xue, C. Wei, X. Zhang, S. Liang, X. Wang, X. Huang, Techno-economic characteristics of wastewater treatment plants retrofitted from the conventional activated sludge process to the membrane bioreactor process, Front. Environ. Sci. Eng. 16 (2022), https://doi.org/10.1007/s11783-021-1483-6.
[35] T. Fudge, I. Bulmer, K. Bowman, S. Pathmakanthan, W. Gambier, Z. Dehouche, S. M. Al-Salem, A. Constantinou, Microbial electrolysis cells for decentralisedwastewater treatment: the next steps, Water (Switzerland) 13 (2021), https://doi.org/10.3390/w13040445.